J. Biochem. **141,** 513–524 (2007)
doi:10.1093/jb/mvm053

Human Xanthine Oxidase Changes its Substrate Specificity to Aldehyde Oxidase Type upon Mutation of Amino Acid Residues in the Active Site: Roles of Active Site Residues in Binding and Activation of Purine Substrate

Yuichiro Yamaguchi[1,2], Tomohiro Matsumura[1], Kimiyoshi Ichida[2], Ken Okamoto[1] and Takeshi Nishino[1,*]

[1]Department of Biochemistry and Molecular Biology, Nippon Medical School, 1-1-5 Sendagi, Bunkyo-ku, Tokyo 113-8602, Japan; and [2]Division of Kidney and Hypertension, Department of Internal Medicine, Jikei University School of Medicine, 3-25-8 Nishishinbashi, Minato-ku, Tokyo 105-8461, Japan

Received December 28, 2006; accepted January 28, 2007; published online February 14, 2007

Xanthine oxidase (oxidoreductase; XOR) and aldehyde oxidase (AO) are similar in protein structure and prosthetic group composition, but differ in substrate preference. Here we show that mutation of two amino acid residues in the active site of human XOR for purine substrates results in conversion of the substrate preference to AO type. Human XOR and its Glu803-to-valine (E803V) and Arg881-to-methionine (R881M) mutants were expressed in an *Escherichia coli* system. The E803V mutation almost completely abrogated the activity towards hypoxanthine as a substrate, but very weak activity towards xanthine remained. On the other hand, the R881M mutant lacked activity towards xanthine, but retained slight activity towards hypoxanthine. Both mutants, however, exhibited significant aldehyde oxidase activity. The crystal structure of E803V mutant of human XOR was determined at 2.6 Å resolution. The overall molybdopterin domain structure of this mutant closely resembles that of bovine milk XOR; amino acid residues in the active centre pocket are situated at very similar positions and in similar orientations, except that Glu803 was replaced by valine, indicating that the decrease in activity towards purine substrate is not due to large conformational change in the mutant enzyme. Unlike wild-type XOR, the mutants were not subject to time-dependent inhibition by allopurinol.

Key words: xanthine oxidoreductase, aldehyde oxidoreductase, molybolenum cofactor, molybdenum, hydroxylase, human xanthine oxidase, allopurinol, xanthinuria.

Abbreviations: AFR25, activity to flavin ratio; AO, aldehyde oxidase; KPB, potassium phosphate buffer; MoCo, molybdopterin cofactor; XDH, xanthine dehydrogenase; XO, xanthine oxidase; XOR, xanthine oxidoreductase.

The atomic coordinates and structure factors (code 2E1Q) have been deposited in the Protein Data Bank.

INTRODUCTION

Eucaryotic xanthine oxidoreductase (XOR) and aldehyde oxidase (AO) both contain a molybdenum cofactor, two iron sulphur clusters and FAD as prosthetic groups (*1–3*). These dimeric proteins are composed of an identical subunit with a molecular mass of about 145 kDa. Hydroxylation of aldehyde and purine substrates can be catalyzed at the molybdenum site in both AO and XOR, but AO catalyzes the reaction of aldehyde more efficiently (*3–6*). On the other hand, purines such as hypoxanthine and xanthine are good substrates for XOR, but poor substrates for AO. Furthermore, allopurinol (4-hydroxypyrazolopyrimidine) inhibits XOR (*7*), but not AO (*8*). Interestingly, allopurinol is a substrate for both enzymes (*8*, *9*).

Inherited xanthinuria involving abnormalities of these enzymes has three subtypes: classical xanthinuria type I, which is due to XOR deficiency; classical xanthinuria type II, which is due to deficiency of both XOR and AO; and xanthinuria type III, which is due to molybdenum cofactor deficiency (*10*). Most patients with classical xanthinuria type I or type II have no symptoms, but some patients may develop urinary tract calculi, acute renal failure or myositis due to tissue deposition of xanthine (*10*). Molybdenum cofactor deficiency is associated with severe neurological disorders caused by sulphite oxidase deficiency, and clinical treatment is usually focused on these disorders (*11*). Classical xanthinuria (types I and II) can be easily differentiated by means of the allopurinol-loading test (*8*). As allopurinol is converted to oxypurinol (4,6-dihydroxypyrazolopyrimidine) by both XOR and AO, oxypurinol is detected in urine and serum of patients with classical xanthinuria type I upon administering allopurinol, but not in urine or serum of patients with type II (*8*).

*To whom correspondence should be addressed. Tel: +81-3-3822-2131, Fax: +81-3-5685-3054, E-mail: nishino@nms.ac.jp

The reaction catalyzed by the Mo hydroxylases is distinct from those of other biological hydroxylation systems, such as P450, in that an oxygen atom is incorporated into the product from water, rather than an O_2 molecule (*2*). In the oxidized enzyme, the metal is in the Mo(VI) oxidation state, bearing an oxo (=O), one hydroxo (OH) and a sulphido ligand (*2*). In the course of a single turnover, the oxygen atom at the catalytically labile site on the Mo centre is transferred to the substrate and subsequently the labile site is regenerated by oxygen derived from the solvent prior to a second turnover (*12*). Exchangeability of the two groups (=O, –OH), including the catalytically labile site, during the reaction and the overall reaction mechanism have been the topics of recent studies (*13–17*). Hille and co-workers (*18*) carried out single-turnover experiments by pursuing the incorporation of ^{17}O into XO and demonstrated that it is Mo–OH rather than Mo=O that is catalytically labile. It was proposed that Glu1261 acts as an active-site base initiating the catalytic reaction that abstracts a proton from the Mo–OH group, which then nucleophilically attacks the substrate carbon atom to be hydroxylated. In addition, on the basis of the crystal structure of aldehyde oxidoreductase from *Desulfovibrio gigas*, a mechanism of aldehyde hydroxylation was proposed that involves similar chemistry (*19*). The crystal structure of bovine XOR complexed with an intermediate in the hydroxylation reaction of the slow-reacting substrate FYX-051 has been solved recently (*20*), and it was shown that the catalytically labile Mo–OH oxygen forms a bond with a carbon atom of the substrate, supporting fully the reaction mechanism described earlier. In addition, the Mo=S group of the oxidized enzyme is protonated to afford Mo–SH upon reduction of the molybdenum centre and this last ligand unambiguously occupies an equatorial position in the square-pyramidal metal coordination sphere, appropriate for hydride transfer from the substrate carbon atom to the Mo=S group. In this structure, Glu1261 can act as a general base by abstracting the proton from Mo-OH, and the newly protonated Glu1261 is stabilized by hydrogen bond formation with the N-1 nitrogen of the substrate (*20*). Mutation of the corresponding residue Glu730 in *Rhodobacter capsulatus* xanthine dehydrogenase (XDH) resulted in loss of hydroxylation activity (*21*). In the crystal structure of the FYX-051-bound form, protonated Glu802 is hydrogen-bonded with the nitrogen atoms of the substrate (*20*), indicating the importance of this residue for binding of heterocyclic substrates.

In this study, we expressed human XOR in an *Escherichia coli* system and examined the effect of mutation of active-site amino acids on the balance of XOR and AO activities in order to obtain basic knowledge that might be relevant to clinical diagnosis as described earlier, and to establish the roles of these amino acid residues in the substrate activation mechanism at the molybdenum centre.

EXPERIMENTAL PROCEDURES

Materials—The restriction and modification enzymes were obtained from Takara Bio (Ohtsu, Japan). Preswollen DE-52 anion exchange resin was purchased from Whatman (NJ, USA) and hydroxyapatite gel from Bio-Rad Laboratory (CA, USA).

Bacterial Strains and Plasmids—Plasmid pTrcHXDH, which was designed for overexpression of human XOR, and its derivatives were used to transform the *E. coli*, strain JM109. The plasmid pTrcHXDH was used as a template for site-directed mutagenesis. Mutagenesis was performed using a QuickChange™ site-directed mutagenesis kit (Stratagene, CA, USA). Cultures were grown with shaking at 37°C (preculture) or 30°C (expression) in Luria-Bertani broth. Ampicillin (50 μg/ml), sodium molybdate (1 mM), and isopropyl-β-D-thiogalactopyranoside (50 μM) were used as required.

Plasmid Construction and Mutagenesis—The cDNA of human XOR (*22*) was cloned from a human liver cDNA library (Takara Bio, Ohtsu, Japan) by PCR. The primers using for PCR were as follows: HXDHP5, 5′-TGA TCA TGA CAG CAG ACA AAT TGG TT-3′, HXDHP4, 5′-TCT AGA TCT TTA GAC CCT CAC AGA CCA GGG-3′. The PCR fragment was partially digested with BspHI/XbaI, and fragments of about 4 kbp were cloned into the NcoI/XbaI site of the expression vector pTrc99A; the resulting vector was designated pTrcHXDH. Mutagenic oligonucleotide primers were as follows: E803Vfp, 5′-GGC TTT GGA GGC AAG GTG ACC CGG AGC ACT GTG-3′, and E803Vrp, 5′-CAC AGT GCT CCG GGT CAC CTT GCC TCC AAA GCC-3′, R881Mfp, 5′-TCT CAG AGT ATT ATG GAA ATG GCT TTA TTC CAC ATG GAC-3′, R881Mrp, 5′-GTC CAT GTG GAA TAA AGC CAT TTC CAT AAT ACT CTG AGA-3′. Mutagenesis reactions were carried out according to the kit manufacturer's instructions. The resulting DNA prepared from individual colonies was sequenced to verify the presence of the desired mutations. DNA sequencing was performed with an ABI PRISM 310 Genetic Analyzer using a BigDye® Terminator Cycle Sequencing Ready Reaction sequencing kit (Applied Biosystems, CA, USA).

Overexpression of Recombinant XOR—Escherichia coli JM109 transformed with pTrcHXDH was grown overnight at 37°C in 5 ml of Luria–Bertani broth containing 50 μg/ml ampicillin and 1 mM sodium molybdate. Cells were then subcultured into 100 ml of the same medium. When cell growth had reached the medium log phase, these cultures were used to inoculate 2 l baffled flasks containing 700 ml of the same medium. Flasks were shaken at 30°C, and expression was induced by addition of 50 μM isopropyl-β-D-thiogalactopyranoside. Cells were harvested by centrifugation, and stored at –80°C until required.

Purification of Enzymes—All steps of the purification procedure were performed at 4°C. Cells (about 10 g wet weight) were suspended in 40 ml of 20 mM Tris–HCl buffer, pH 8.5, containing 0.5 mM EDTA, 0.2 mM PMSF and 0.5 mg/ml of lysozyme. The cell suspension was disrupted by sonication on ice. After centrifugation at 100,000*g* for 30 min, the supernatant was applied to a column of DE-52 (2.5 cm × 16 cm) equilibrated in 20 mM Tris–HCl buffer, pH 8.5, containing 0.5 mM EDTA and 1 mM sodium salicylate. The column was washed with 50 ml of equilibration buffer, and the enzyme was eluted from the column with a linear gradient of 0–300 mM NaCl containing equilibration buffer. The

XOR fraction was applied to a column of hydroxyapatite gel (1.5 cm × 2.5 cm) equilibrated with 50 mM potassium phosphate buffer (KPB), pH 7.8. The column was washed with 20 ml of 50 mM KPB, pH 7.8, and the enzyme was eluted with a linear gradient of 50–500 mM KPB, pH 7.8. The active XOR fraction was pooled and concentrated using a Centriprep YM-50 or a Centricon YM-100 (Millipore, MA, USA). The enzyme sample was applied to a gel filtration column (Superdex 200pg, 1.5 cm × 45 cm, Amersham Bioscience, Uppsala, Sweden) equilibrated with 50 mM Tris–HCl buffer, pH 8.5, containing 1 mM sodium salicylate and 0.1 mM EDTA. Then, the active fraction was pooled and used for kinetic analysis. The concentration of purified enzymes was determined from the absorbance at 450 nm using an extinction coefficient of 35.8 mM^{-1} cm^{-1} (*23*).

SDS-polyacrylamide Gel Electrophoresis—SDS-PAGE was performed as described by Laemmli (*24*) using 10% polyacrylamide gel. The gels were stained with Coomassie Brilliant Blue R.

Enzyme Assays—Enzyme assays were carried out at 25°C in Tris buffer (50 mM, pH 8.5) in a final volume of 3 ml. All samples were temperature-controlled at 25°C. For the steady-state kinetics analysis using hypoxanthine or xanthine as a substrate, the reaction solution was 3 ml of Tris buffer, containing various concentrations of substrate (for the wild-type, the xanthine or hypoxanthine concentration range was 5–150 μM; for the mutants, it was 100–500 μM). In order to minimize the effect of the inactive-form enzymes that could potentially bind substrates, the enzyme assays were performed under conditions where the total enzyme concentration was less than 1/100 of the substrate concentration. Total enzyme concentrations (determined from the absorbance at 450 nm) were within the ranges of 10–30 and 50–200 nM for the wild-type and mutant enzymes, respectively. The reaction was started by mixing the enzyme with the substrate solution and the activity was followed photometrically for 5 min to obtain the initial velocity. When the substrate was xanthine, substrate oxidation activity was measured as change of absorbance at 295 nm due to urate formation. When the substrate was hypoxanthine, the change of absorbance at 285 nm was measured. For the steady-state kinetics using benzaldehyde or *p*-(dimethyamino)cinnamaldehyde as a substate, the reaction solution was 3 ml of Tris buffer, containing various concentrations of substrate (benzaldehyde 1–100 μM, *p*-(dimethyamino)cinnamaldehyde 0.5–40 μM). For these assays we used 100 μM 2,6-dichlorophenolindophenol (DCPIP) as an electron acceptor, which receives an electron from the Mo centre directly regardless of XDH or XO form, and reduction of DCPIP was measured in terms of absorbance change at 600 nm using an extinction coefficient of 20 mM^{-1} cm^{-1} according to the reported method (*25*), with some modification. Total enzyme concentrations used (determined at 450 nm) were of 40 nM and 20 nM for the wild-type and the mutant enzymes, respectively. Under these conditions, the effect of inactive-form enzymes that could potentially bind substrates would result in an error of less than 10% in the parameter values. Absorbance spectra were recorded with a Shimadzu UV-2550 dual-wavelength double-beam spectrophotometer (Shimadzu, Kyoto, Japan).

Crystallization and Data Collection of the E803V Mutant of XOR—The E803V mutant was purified as described earlier, and the enzyme, containing both active and inactive forms, was concentrated to 15 mg/ml in 5 mM Tris buffer (pH 8.5) containing 1 mM sodium salicylate and 0.1 mM EDTA. The enzyme was incubated with 5 mM dithiothreitol for 1 h at room temperature. Aliquots of 5 μl of dithiothreitol-treated enzyme solution were mixed with 5 μl of 100 mM sodium citrate buffer (pH 5.0) containing 8–11% polyethylene glycol 8000, 5 mM dithiothreitol, 1 mM sodium salicylate, 0.1 mM EDTA, and placed on siliconized glass plates. Crystals were grown for 7 days at 20°C. The crystals were mounted on a nylon loop, and stored in liquid nitrogen. Diffraction data were collected at Photon Factory (KEK, Tsukuba, Japan) beamline NW12A, and SPring-8 (JASRI, Hyogo, Japan) beamline BL38B1. Data were reduced with the help of the program package HKL2000 and scaled using SCALEPACK. Ramachandran statistics indicate the fractions of residues in the most favored, additionally allowed, generously allowed, and disallowed regions of the Ramachandran diagram as defined by the program PROCHECK (*25*). The program package EPMR (*26*) established the correct solutions of the respective molecular replacement function (20.0–4.0 Å resolution range). Bovine milk XDH (Protein Data Bank code 1FO4) without its cofactors was employed as a search model. The molecular models were built with the help of the program package O (*27*). Subsequent refinement, including rigid body, simulated annealing, grouped B factors, and least-squares minimization were carried out with CNS, version 1.0 (*28*).

RESULTS

Expression of Recombinant Human XOR—The only heterologous expression system of mammalian XOR so far reported is a baculovirus expression system (*29*, *30*). An attempt to obtain rat liver XOR using the same *E. coli* system was unsuccessful, because the protein was expressed as insoluble inclusion bodies (data not shown). However, when cDNA of human XOR was cloned into expression vector pTrc99A and expressed in the *E. coli* system, the recombinant protein was obtained as a soluble, active form, which could be purified by column chromatography, as described in the section 'EXPERIMENTAL PROCEDURE'. The molecular mass of the purified protein was calculated to be approximately 150 kDa from the results of SDS-PAGE (Fig. 1A), while a value of approximately 300 kDa was obtained from gel filtration chromatography (data not shown). These data indicate that the recombinant protein was a homodimer, as is generally the case for mammalian XORs. The visible absorption spectrum of the recombinant enzyme was similar to those of other mammalian XORs, except for the region around 320 nm (Fig. 1B). The absorbance ratio of A280/A450 was similar to those of other mammalian XORs (data not shown).

The activity-to-flavin ratio (AFR 25°C) value of the recombinant enzyme ranged between 4 and 20 ($n = 8$), much lower than the corresponding value for fully active bovine milk XOR (*7*). To examine the ratio of active/inactive enzyme, the reduction of recombinant human

XOR by a substrate was analysed under anaerobic conditions. It was found that the purified enzyme (AFR25 = 8.2) was reduced in biphasic manner by xanthine as in the case of bovine milk enzyme (*31*), but the rapid phase was only 4%, indicating that the enzyme contains a large amount of the demolybdo- or desulpho-form of inactive enzyme (*29*). The absorption maximum at 320 nm observed for recombinant XOR (Fig. 1B) resembles that in the spectrum of the demolybdo form of recombinant rat XOR. The content of molybdenum was measured by ICP-MS analysis (data not shown), and the ratio of molybdenum to FAD was 0.36. These results suggested that recombinant human XOR had been expressed mainly as a mixture of inactive demolybdo and desulpho forms. The specific activity, however, can be determined as the turnover number from the content of active enzyme, which was determined by means of a rapid reduction experiment with substrate. The steady-state kinetics of recombinant XOR is shown in Table 1. The K_m value of the recombinant protein in xanthine hydroxylation assay was similar to previously reported values (*31*, *32*). The k_{cat} value of the recombinant enzyme based on the amount of active enzyme was similar to those of other mammalian XORs. The k_{cat} of fully active XOR prepared from bovine milk was about $\sim$1000 min^{-1}. Krenitsky *et al*. (*33*) reported the characteristics of human XOR purified from liver; the specific activity of the liver XOR was 1.8 U/mg protein (k_{cat} = $\sim$270 min^{-1}), suggesting that their enzyme also consisted mainly of inactive form(s) of the enzyme, as is usual in natural XOR preparations. Although the content of the active enzyme in the expressed enzyme proteins is low due to low molybdenum and sulphur incorporation, it is still possible to compare the substrate specificities for hypoxanthine, xanthine and aldehydes, and to examine the roles of amino acid residues in the active site and the mechanisms of substrate recognition and activation by using similarly prepared wild-type and mutant enzymes, since the enzymes can be obtained in relatively large amounts and the activity can be determined accurately.

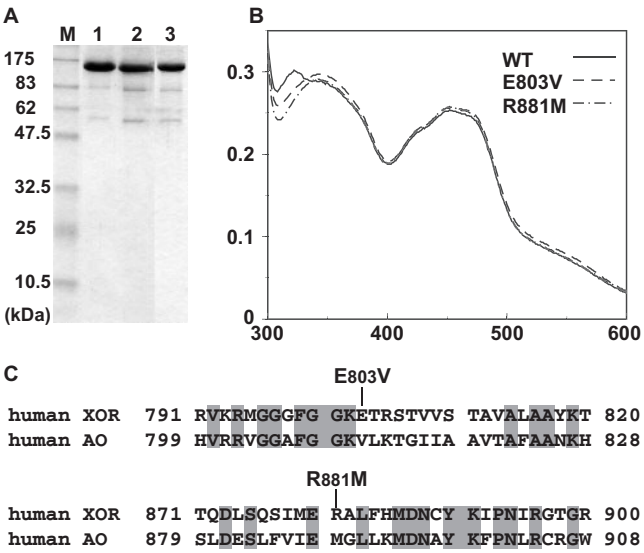

Fig. 1. **Purification of recombinant XOR and its mutants.** (A) Purified enzymes were analysed by 10% SDS-PAGE. Each lane contained 2.5 μg of purified enzyme: lane 1, recombinant human XOR (wild type), lane 2, E803V mutant; lane 3, R881M mutant; M, molecular weight standard. (B) Absorption spectra of recombinant XORs. Spectra were recorded at the concentration of 7.1 μM. (C) The amino acid sequence of human XOR (*22*) around the mutation site is aligned with that of human AO (*34*).

Mutation of Glu803 and Arg881 Residues of Human XOR and Crystal Structure of E803V Mutant of Human XOR—Aldehyde oxidase (AO) shows significant homology with XOR. The amino acid sequence of human AO is about 50% identical with that of human XOR (*3*, *34*). There are some differences of the molybdopterin cofactor (MoCo) domain between XOR and AO at the substrate binding site, and Glu803 and Arg881 are only conserved in XORs (Fig. 1C). These residues are located around the substrate-binding site and are likely to have important role(s) in the recognition and/or activation of substrate. The tertiary structures of bovine XOR at the MoCo site have been determined in the complexes with salicylate (*35*), and FYX-051 (Fig. 2A) (*20*) or TEI-6720 (*36*). The Glu803 of human XOR, corresponding to Glu802 of bovine XOR, is associated with the apical oxygen atom of MoCo via a hydrogen bond in the structure of the salicylate-bound form. When the substrate analogue binds to the MoCo centre, the side chain of Glu803 swings out to form a hydrogen bond with the nitrogen atom of the inhibitor TEI-6720 (*36*) or FYX-051 (*20*). In the latter structure Glu803 is considered to be obligatorily protonated to form a hydrogen bond with the nitrogen atom. The Arg881 residue, corresponding to Arg880 of the bovine enzyme, is associated with oxygen of the substrate via a hydrogen bond in the salicylate-bound structure and with the oxygen atom of the 6-position of oxypurinol (ref. Fig. 6C) in the crystal structure of the oxypurinol-bound form of reduced XDHs from *R. capsulatus* (*37*) and bovine milk (Egar,

Table 1. **Steady-state kinetic parameters of the recombinant enzymes for purine hydroxylation.**

	Xanthine			Hypoxanthine		
	K_m (μM)	k_{cat} (min^{-1})[a]	k_{cat}/K_m (μM^{-1} min^{-1})	K_m (μM)	k_{cat} (min^{-1})[a]	k_{cat}/K_m(μM^{-1} min^{-1})
WT	8.8 ± 0.60	1100 ± 52	130 ± 7.0	1.7 ± 0.02	1800 ± 130	1000 ± 90
E803V	72 ± 10	81 ± 7.2	1.1 ± 0.11	n.d.[c]	n.d.[c]	–
R881M	n.d.[b]	n.d.[b]	–	21 ± 1.5	20 ± 1.4	0.94 ± 0.04

[a]The k_{cat} values were corrected for the amount of active enzyme determined by reduction of the enzymes with hypoxanthine under anaerobic conditions.
[b]The xanthine hydroxylation activity of the R881M mutant was negligible, so the K_m and k_{cat} values could not be determined.
[c]The hypoxanthine hydroxylation activity of the E803V mutant was negligible, so the K_m and k_{cat} values could not be determined.

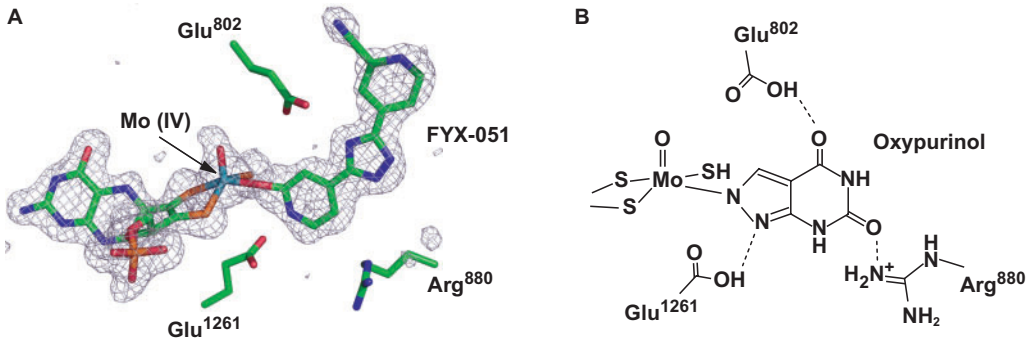

Fig. 2. **The structure of inhibitor-bound complex at the active site of bovine XOR.** (A) Shown are the electron density map of MoCo and the inhibitor molecule FYX-051 (*20*), and the side chains of amino acid residues interacting with the inhibitor. (B) Model of the oxypurinol complex at the active site of *R. capsulatus* XDH (*37*) and bovine XOR (Egar, B.T., Pai, E.F., Okamoto, K. and Nishino, T., unpublished observation).

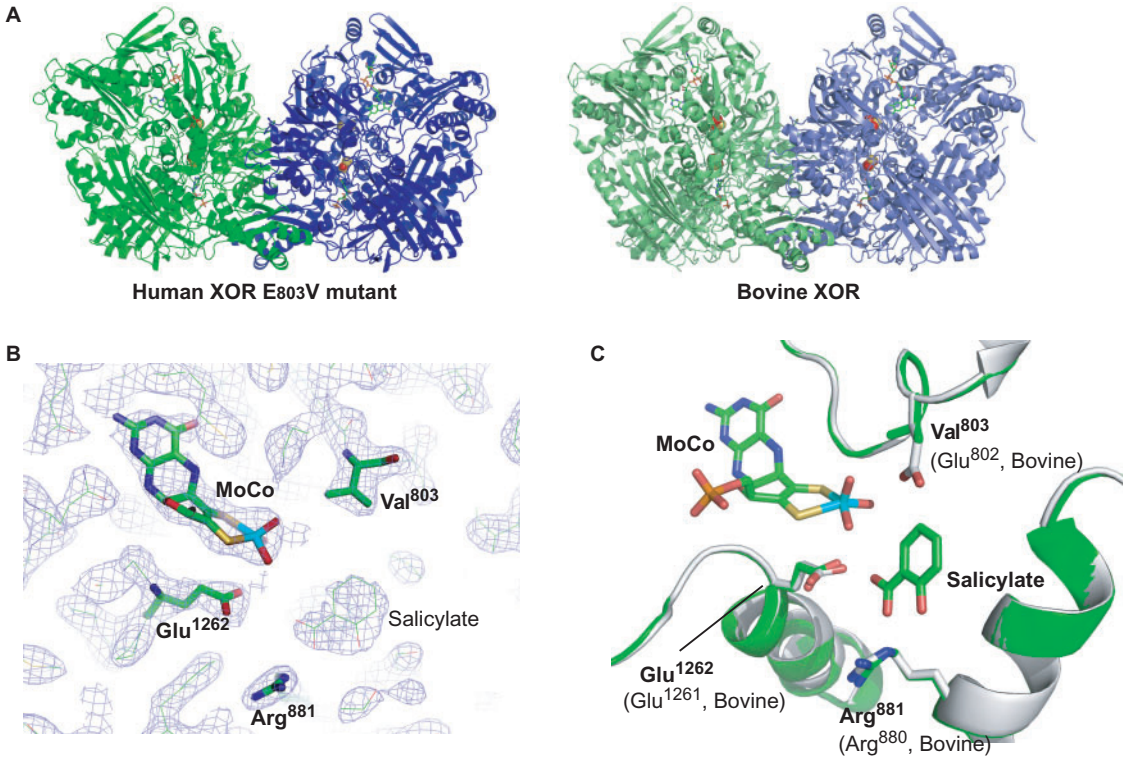

Fig. 3. **Crystal structure of human XOR E803V mutant.** (A) Whole structure of E803V mutant XOR (left) compared with that of bovine XOR (right; *35*; PDB:1FO4). (B) $2F_o$-F_c electron density map around the active site of human XOR mutant. The molybdenum cofactor and three amino acid residues (Val803, Arg881 and Glu1262) are presented in stick models, and the other peptide and salicylate are presented in line models. The atom colours are indicated as follows, C, green; N, blue; O, red; S, yellow; P, orange; Mo, cyan. (C) Superposition of the active site amino acid residues from E803V mutant of human XOR (green) and bovine XOR (gray) in cartoon and stick models. The molybdopterin cofactor and salicylate of the E803V mutant enzyme are shown in stick models.

B.T., Pai, E.F., Okamoto, K., Nishino, T., unpublished observation) as illustrated in Fig. 2B. Therefore, we mutated Glu803 to Val (E803V) and Arg881 to Met (R881M) (Fig. 1C).

The mutants were obtained by using the same procedure as for the wild-type enzyme. The absorption spectra of these mutants were similar to that of the wild-type enzyme, except for the region around 320 nm. In order to confirm that no large conformational changes had occurred in the mutant enzymes, we tried to obtain crystals, and succeeded in crystallizing the E803V mutant. Crystal diffraction data were collected to 2.6 Å resolution, and the structure was determined by molecular replacement techniques with MD refinement (Table 3). The asymmetric unit contains two homodimers, in contrast to the previously characterized bovine milk XDH, the asymmetric unit of which contains only one homodimer. Overall, however, the two

structures are very similar (Fig. 3A). In both cases, the monomer consists of three major domains, the amino-terminal, iron–sulphur centre-binding domain, the FAD-containing intermediate domain and the largest, carboxyl-terminal domain (*1*). The latter corresponds to the molybdopterin-binding domain in bovine milk XDH and the molybdopterin cofactor was present in this mutant structure, suggesting that the enzyme is the desulpho-form. Although we previously reported the crystal structure of the rat mutant enzyme in the demolybo-form (*38*), in this human structure the demolybdo-enzyme might have been excluded during crystallization, in view of the Mo content of the original sample. The overall structure of the molybdopterin domain of this E803V mutant is not greatly different from that of the molybdo-form of bovine milk XDH in salicylate bound-form, and the amino acid residues near the molybdo-pterin cofactor in the active site pocket are situated at very similar positions and in similar orientations, except that Glu803 was replaced with valine (Fig. 3B). The structure of mutant XOR was superimposed with milk XOR (Fig. 3C). A superposition of two structures is calculated using the SuperPose version 1.0 server (*39*). These proteins share 89% sequence identity, and a root mean square deviation (RMSD) for α-carbon of MoCo domain is 0.42 Å. These results indicate that decrease in activity towards purine substrate is not due to any large conformational change in the mutant enzyme.

Purine Oxidation Activity of E803V and R881M Mutants—The activities of mutants towards hypoxanthine and xanthine as substrates were substantially decreased, while the aldehyde oxidation activities were drastically increased, compared with those of the wild-type enzyme (Fig. 4). These results indicate that both the Glu803 and R881 residues are important for catalytic activity towards both hypoxanthine and xanthine substrates, but not aldehyde substrates. Although the remaining activities of both mutants towards hypoxanthine and xanthine substrates were very weak compared with those of the wild-type enzyme, we performed steady-state kinetic analyses of these mutants with xanthine and hypoxanthine substrates. The amounts of active form of the mutants were measured in terms of reduction by hypoxanthine and xanthine under anaerobic conditions, and were similar to that of the wild-type enzyme. The steady-state kinetic parameters of the mutant enzymes are summarized in Table 1. The K_m value of the E803V mutant was eight times larger, and the k_{cat} value was 13 times lower compared with the wild-type enzyme, while the K_m value of R881M was 12 times larger, and the k_{cat} value was 90 times lower. With hypoxanthine as a substrate, it was difficult to detect any activity of the E803V mutant, and therefore, the kinetic parameters were not determined. On the other hand, with xanthine as a substrate, the R881M mutant showed little activity, and the kinetic parameters could not be determined. It should be noted that the K_m values determined are much larger than the total amounts of the enzyme used, so that substrate binding to the inactive enzymes contained in the sample should not have significantly influenced the K_m values determined under these conditions, as described in the section 'EXPERIMENTAL PROCEDURES'. It was reported that the natural Arg881 mutant of *Drosophila* XDH lacked activity (*40*). Here, we found that, although both Glu803 and Arg881 are important for activities towards both hypoxanthine and xanthine substrates, the Arg881 residue is essential for activity towards xanthine, but not hypoxanthine, as a substrate. On the other hand, Glu803 is essential for activity towards hypoxanthine, but not xanthine, as a substrate.

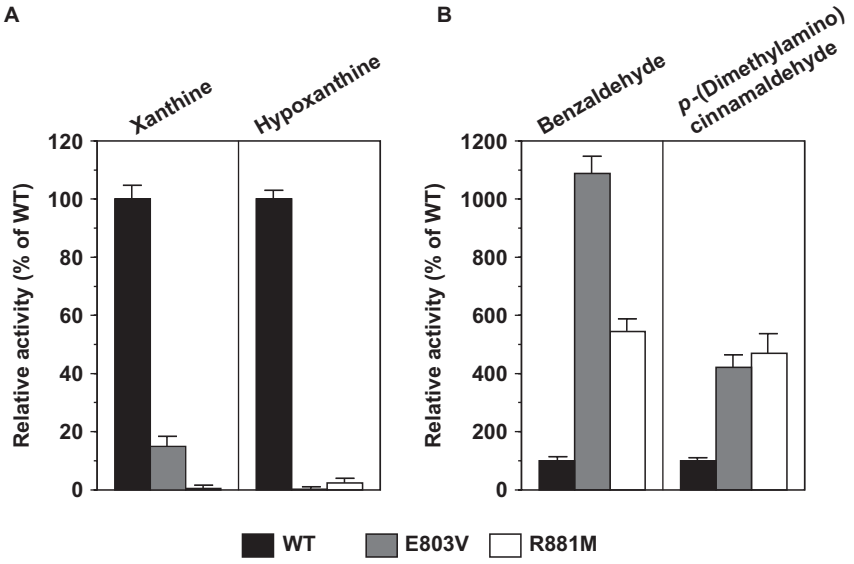

Fig. 4. **Activity of recombinant XORs.** The activity of the recombinant enzyme was assayed in terms of purine oxidation (A) or aldehyde oxidation (B). The relative activity of each enzyme was determined as the initial rate of oxidation of substrate. (A) 50 μM xanthine or hypoxanthine was added to the assay mixture as a substrate. (B) 5 μM benzaldehyde or *p*-(dimethylamino)cinnamaldehyde was added to the assay mixture as a substrate.

Table 2. **Steady-state kinetic parameters of the recombinant enzymes for aldehyde oxidation.**

	Benzaldehyde			*p*-(Dimethylamino)cinnamaldehyde		
	K_m (μM)	k_{cat} (min^{-1})[a]	k_{cat}/K_m($\mu M^{-1}\,min^{-1}$)	K_m (μM)	k_{cat} (min^{-1})[a]	k_{cat}/K_m($\mu M^{-1}\,min^{-1}$)
WT	39 ± 2.0	270 ± 50	7.0 ± 0.6	29 ± 1.5	330 ± 50	11 ± 0.60
E803V	6.2 ± 0.61	130 ± 9.0	22 ± 1.1	0.32 ± 0.091	14 ± 0.70	43 ± 2.1
R881M	18 ± 1.5	730 ± 60	40 ± 1.3	20 ± 0.90	300 ± 25	15 ± 0.80

[a]The k_{cat} values were corrected for the amount of active enzyme determined by reduction of the enzymes with hypoxanthine or xanthine under anaerobic conditions.

Table 3. **Data collection and refinement statistics.**

Space group	$P2_1$
Unit cell axes (Å)	$a = 134.6$, $b = 140.9$, $c = 176.5$
Unit cell angle (°)	$\alpha = \gamma = 90$, $\beta = 91.49$
Resolution range (Å)	50–2.60
Number of unique reflections (used for *R*-free calculation)	192,029 (3,840)
R_{sym}[a]	8.5 (38.7)
$I/\sigma I$	12.2 (3.9)
Completeness (%)	98.2 (92.0)
R_{cryst} (R_{free})[b]	0.192 (0.246)
Rmsd bond length (Å)	0.007
Rmsd bond angles (°)	1.4
Number of non-hydrogen atoms	41,725
Ramachandran plot (%)	87.4, 11.6, 0.8, 0.3

[a]$R_{sym} = \sum_{hkl}\sum_I |I_I - \langle I\rangle| / \sum_{hkl}\sum_I \langle I\rangle$ where I_I is the *i*th measurement and $\langle I\rangle$ is the weighted mean of all measurement of *I*.

[b]$R_{cryst} = \sum_{hkl} |F_{obs} - F_{calc}| / F_{obs}$ where F_{obs} and F_{calc} are the observed and calculated structure factors, respectively, and the summation is over the reflections used for model refinement. R_{free} was the same as R_{cryst} for 2.0% of the data randomly omitted from the total data.

Values in parentheses refer to the highest resolution shell (2.64–2.60 Å).

Ramachandran statistics indicate the fractions of residues in the most favoured, additionally allowed, generously allowed, and disallowed regions of the Ramachandran diagram as defined by the program PROCHECK (*25*).

Activity of Mutant XORs for Aldehyde Oxidation—The steady-state kinetics of mutant XORs for aldehyde substrate are shown in Table 2. We used benzaldehyde and *p*-(dimethylamino)-cinnamaldehyde as typical AO electron donor substrates and dichlorophenol indophenol as an electron acceptor which receives an electron via Mo regardless of XDH or XO form (*23*, *32*) in order to understand the roles of the amino acid residues 803 and 881 in the hydroxylation reaction of aldehyde at the molebdenum centre. The K_m value of the E803V mutant was drastically decreased, while the k_{cat} value was also decreased. The K_m value of the R881M mutant was not much changed, though the k_{cat} value was increased. These data indicate that the affinity for aldehyde was affected by the E803V mutation, and the turnover of aldehyde was affected by the R881M mutation. The substrate specificity of XOR may be changed completely to the AO type by the double mutation of E803V/R881M, which should result in no activity towards purine substrates, whereas high activity towards aldehyde substrates can be expected. We tried to express the E803/R881M double mutant of XOR in the *E. coli* system, but only a negligible amount was expressed and the protein could not be isolated (data not shown).

Effect of Allopurinol on the Purine Oxidation by Mutant XORs—Allopurinol is an inhibitor of mammalian XORs. The inhibitory effect of allopurinol on XOR is known to be potent and time-dependent (*7*), and is due to the tight binding of oxypurinol, the oxidized form of allopurinol generated by reaction with XOR, to the reduced form of the molybdenum cofactor of XOR. However, the inhibitory effect of allopurinol on the purine oxidation reaction by AO is very weak (*8*, *41*). The effect of allopurinol on purine oxidation by recombinant XORs is shown in Fig. 5. The oxidation reaction of xanthine by the wild-type enzyme was completely inhibited by allopurinol (Fig. 5A and B), while the reactions catalyzed by the E803V mutant was not inhibited, though these reactions are slow compared with those of the wild-type enzyme, due to mutation, as shown in the Table 1 (Fig. 5C). The apparent rate of hypoxanthine oxidation by the R881M enzyme was slight (Fig. 5D), but the rate of absorbance increase at 285 nm accelerated rather than stopping, apparently due to allopurinol oxidation by the mutant: it is likely that the R881M mutant oxidized hypoxanthine and allopurinol to xanthine and oxypurinol, respectively, and that the change in absorbance at 285 nm reflected the accumulation of both xanthine and oxypurinol. These results indicate that the mutations in the active site of XOR made the inhibitor ineffective. This would be consistent with the lack of effect of allopurinol on the activity of AOs. The formation of a tight binding complex of the Mo atom of XOR with oxypurinol would be stabilized by hydrogen-bonding with the three amino acids previously mentioned. The crystal structures of oxypurinol-bound *R. capsulatus* XDH as well as bovine XOR support this view.

DISCUSSION

Eucaryotic XOR and AO are similar in protein structure and prosthetic group composition, but are different in substrate preference. Both XOR and AO contain a molybdenum cofactor, two iron sulphur clusters and FAD as prosthetic groups (*1–3*). Although the two enzymes are similar, they have different characteristics of substrate specificity at the molybdenum centre, as well as the FAD centre. Hydroxylation of aldehyde and purine substrates can be catalyzed at the molybdenum centre in

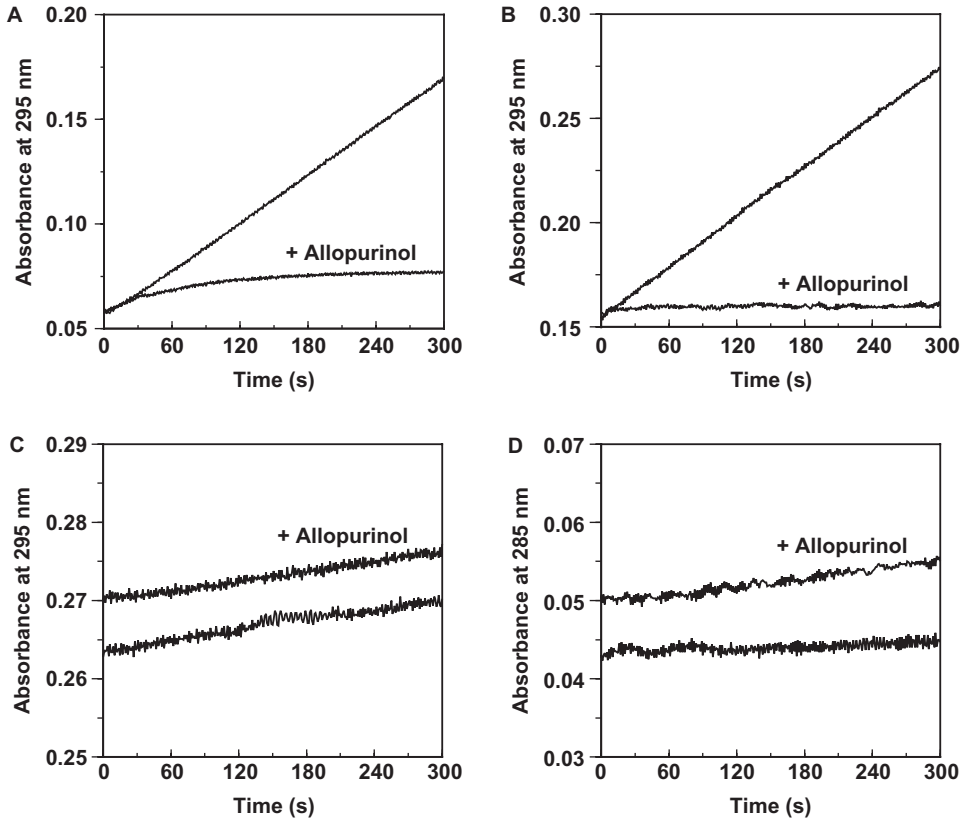

Fig. 5. **The effect of allopurinol on the purine oxidation reaction.** The oxidation of xanthine or hypoxanthine was measured under standard conditions. The reaction was started by adding about 150 nM XOR (A) and (B), or 300 nM E803V (C), or 300 nM R881M (D). The reaction mixture contained: (A) 100 μM xanthine with (10 μM) or without allopurinol. (B) 150 μM xanthine with (100 μM) or without allopurinol. (C) 300 μM xanthine with (100 μM) or without allopurinol. (D) 300 μM hypoxanthine with (100 μM) or without allopurinol.

both AO and XOR, but AO catalyzes the reaction of aldehyde more efficiently (*3*–*6*). On the other hand, purines such as hypoxanthine and xanthine are good substrates for XOR, but poor substrates for AO.

At the FAD centre, O_2 is always the electron acceptor of AO, but NAD^+ is a natural substrate for the XDH form of XOR, and it is replaced by O_2 for the XO form in mammalian XOR generated by disulphide formation or proteolytic nicking of the protein molecule. The mechanism of conversion of XDH to XO is well understood, owing to recent advances in crystallographic and site-directed mutagenesis studies (*38*). In the present study, we expressed human XOR in an *E. coli* system and examined the effect of mutation of active-site amino acids on the balance of XOR and AO activities in order to establish the roles of these amino acid residues in the substrate activation mechanism at the molybdenum centre.

This is the first report of an expression system for mammalian XOR in *E. coli*. In the case of bacterial XDH, almost fully active enzyme can be expressed in *E. coli* in sufficient amounts for detailed analysis of the mechanism of molybdenum hydroxylation by means of spectroscopic methods (*21*, *42*). The cDNA of human XOR was cloned into expression vector and expressed in the same expression system of bacterial XDH. The recombinant protein was obtained as the active form, though the content of active form of recombinant human XOR was lower than that of recombinant bacterial XDH. The presence of the inactive forms has been known as desulpho-form or demolybdo-form in the natural bovine milk (*43*), chicken (*44*), rat liver (*32*) and human milk (*45*) XORs. Although the contents are varied presumably depend on the diet conditions in addition to the storage conditions of the enzyme (*43*, *46*), it is possible to obtain the fully active enzyme by means of two steps of affinity chromatography (*47*). The specific activity of recombinant human XOR was increased by the purification using the first folate affinity column chromatography (data not shown). However, further purification with the second affinity column chromatography, to remove the inactive enzyme, cannot be applied to the mutant enzyme, because allopurinol does not bind to the mutant enzyme, as described subsequently.

The conditions for heterologous expression of human sulphite oxidase, a molybdenum cofactor-containing enzyme, have been optimized (*48*). The *E. coli* strain TP1000 was used for high-level expression of human sulphite oxidase, and about 80% of the recombinant enzyme contained the molybdenum cofactor. Although sulphite oxidase does not contain an essential sulphur ligand, as XOR and AO do, we attempted to express

human XOR in TP1000 cells to examine the efficiency of the expression system. Recombinant XOR was obtained from TP1000 cells as well as JM109 cells. However, the AFR value of the purified enzyme ranged between 5 and 40 ($n = 10$), and the ratio of molybdenum to FAD was 0.42 by ICP-MS analysis. These results indicate that over 80% of the recombinant XOR exists in inactive (mixture of desulpho- and demolybdo-) form even in the product expressed in TP1000 cells. Attempts at co-expression of mammalian XOR with XdhC protein in an *E. coli* system, as reported for bacterial XOR (*49*), have not so far been successful in our laboratory. As human molybdenum cofactor sulphurase is essential to generate active sulpho-enzyme in humans (*50*), it may be necessary to co-express this protein in the *E. coli* system to obtain active human XOR, and studies along this line are continuing in our laboratory. Although the specific activity of our human XOR is low, the determination of activity is sensitive enough to permit steady-state kinetics analysis under conditions where the total enzyme concentration (including inactive forms) is much lower than substrate concentration. Furthermore, the amount of active enzyme can be estimated from the extent of rapid bleaching of absorbance at 450 nm of the difference spectra before and after addition of substrate under anaerobic conditions to calculate the turnover number as in the case of natural enzymes (*31*).

The present findings show that mutation of two amino acid residues in the molybdopterin domain of human XOR results in conversion of the electron donor substrate specificity to AO type. Human XOR and its Glu803-to-valine (E803V) and Arg881-to-methionine (R881M) mutants were expressed in an *E. coli* system. The E803V mutant almost completely lost activity towards hypoxanthine as a substrate, but retained very low activity towards xanthine; the K_m value for xanthine was increased eight times and the k_{cat} value was decreased to 7.4% compared with those of wild-type XOR. On the other hand, the R881M mutant lost activity towards xanthine, but retained slight activity towards hypoxanthine; the K_m value for hypoxanthine was increased 12 times and the k_{cat} value was decreased to 1.1% compared with those of wild-type XOR. Both mutants, however, exhibited significant aldehyde oxidase activity. The present experiments show that these differences of substrate preference between XOR and AO reflect different roles of these residues in substrate recognition and activation. Based on the tertiary structure of bovine XOR, the guanidino group of Arg881 may form a hydrogen bond with xanthine, but not hypoxanthine. In the substrate–XOR complex, the side chain of Glu803 may swing out to interact with both xanthine and hypoxanthine by hydrogen bonding. In the light of the mechanistic and structural similarities between bovine or human XOR and *R. capsulatus* XDH, it appears that residue Glu1261 of the bovine enzyme, corresponding to Glu1262 and Glu730 in human and the *R. capsulatus* enzyme, respectively, is essential for activity. It has been reported that mutation of Glu730 in *R. capsulatus* XDH resulted in complete loss of catalytic activity (*21*) and it was also confirmed in this study that the mutation of Glu1262 to alanine in the human enzyme resulted in complete loss of catalytic activity (data not shown); these results are consistent with an essential catalytic role for this residue, which may function as an active-site base to abstract the proton from the Mo-OH group as suggested by Huber *et al*. (*19*) (Fig. 6), leading to nucleophilic attack on the C-8 position of xanthine as a substrate, followed by hydride transfer (*20*, *21*) to give the intermediate (Fig. 6A, IV). Such a reaction intermediate was seen in the crystal structure of the complex of bovine XOR with a slow substrate, FYX-051 (Fig. 2A; *20*), in which the product is directly coordinated to the Mo(IV) centre. It should be noted that, in the crystal structure of the bovine XOR and FYX-051 complex, protonated Glu1261 (after the proton has been abstracted from Mo–OH) forms a hydrogen bond with nitrogen. Such a hydrogen bond should facilitate nucleophilic attack at the carbon atom to be hydroxylated. For xanthine as a substrate, Glu803 and Arg881, as well as Glu1262, can facilitate the nucleophilic attack by forming hydrogen bonds as illustrated in Fig. 6A. In the case of hypoxanthine, Arg881 may not play such a role in hydrogen bond network, in view of the results of our mutation study (Fig. 6B). As regards AO activity, the carbonylated carbon atom of aldehyde can be easily attacked nucleophilically without activation of the substrate by a hydrogen bond network, in contrast to the case of purine substrates. Although we cannot offer any unequivocal explanation for the increase of activity towards the aldehyde substrates used at the moment, it is possible that the E803V mutant may increase the basicity of Mo–O^- via loss of interaction of Glu803 carboxylate with the Mo ligand, if present. Upon binding of purine substrate, this residue swing out to allow hydrogen bond formation with the purine substrate. Indeed, the K_m values of the E803V mutant for aldehyde substrates were decreased significantly compared with those of wild-type XOR. However, this was not the case for the R881M mutant. Thus, it is likely that replacement of the hydrophilic moieties with hydrophobic residues may also contribute to the change of both the affinity for hydrophobic substrates and the velocity of release of the products. Furthermore, inherited xanthinuria involving abnormalities of these enzymes has three subtypes, including xanthinuria type III, which is due to molybdenum cofactor deficiency. It was proposed that classical xanthinuria type I is due to XOR gene deficiency, whereas classical xanthinuria type II, in which patients lack both XOR and AO activities, is due to a defect of the sulphur ligand of the molybdenum atom, which is essential for catalysis in both XOR and AO (*10*). Indeed, it was subsequently established that mutation in the human XOR gene is responsible for xanthinuria type I (*51*), and mutation in the gene for the molybdenum cofactor sulphurase, which provides the sulphur ligand to the molybdenum atom, is responsible for classical xanthinuria type II (*50*). The present experiments showed that, unlike wild-type XOR, the mutants exhibit significant hydroxylation activity toward allopurinol, as well as aldehyde, without showing tight binding inhibition by oxypurinol. The formation of a tight binding complex of the Mo atom of XOR with oxypurinol would be stabilized by hydrogen-bonding with the three amino acids previously mentioned. The crystal

Fig. 6. **Proposed hydrogen-bonding arrangement of the substrate-bound complex at the active site, and proposed mechanism of the purine oxidation reaction by XOR.** (A) The hydroxylation reaction at the C8 position of xanthine is initiated by base-assisted nucleophilic attack of Mo–OH, with concomitant hydride transfer to the Mo=S group to give the reaction intermediate (IV). (B) The hydroxylation reaction at the C2 position of hypoxanthine occurs in the same way as in the case of the xanthine substrate.

structures of oxypurinol-bound *R. capsulatus* XDH as well as bovine XOR support this view. The present results provide support at the enzyme level for the view that classical xanthinuria can be differentiated by means of the allopurinol-loading test. As allopurinol is converted to oxypurinol even by AO without inhibition of the enzyme, oxypurinol is detected in urine and serum of classical xanthinuria type I patients after administration of allopurinol, but it is not detected in urine or serum of patients with a defect of both XOR and AO (xanthinuria type II) (*8*).

We thank Dr Emil F. Pai, University of Toronto, for valuable discussions and Dr Silke Leimkühler, University of Potsdam, for her generous gifts of TP1000 cells and XdhC gene. This work was supported by Grants-in-Aid (T.N. 11169231, T.M. 16770102) for Science Research on Priority Areas and a Grant-in-Aid (T.N. 09480167) for Science Research from the Ministry of Education, Science, Sports and Culture of Japan.

REFERENCES

1. Hille, R. and Nishino, T. (1995) Flavoprotein structure and mechanism. 4. Xanthine oxidase and xanthine dehydrogenase. *FASEB J.* **9**, 995–1003
2. Hille, R. (1996) The mononuclear molybdenum enzymes. *Chem. Rev.* **96**, 2757–2816
3. Garattini, E., Mendel, R., Romao, M.J., Wright, R., and Terao, M. (2003) Mammalian molybdo-flavoenzymes, an expanding family of proteins: structure, genetics, regulation, function and pathophysiology. *Biochem. J.* **372**, 15–32
4. Morpeth, F.F. (1983) Studies on the specificity toward aldehyde substrates and steady-state kinetics of xanthine oxidase. *Biochim. Biophys. Acta* **744**, 328–334
5. Krenitsky, T.A., Neil, S.M., Elion, G.B., and Hitchings, G.H. (1972) A comparison of the specificities of xanthine oxidase and aldehyde oxidase. *Arch. Biochem. Biophys.* **150**, 585–599
6. Beedham, C. (1985) Molybdenum hydroxylases as drug-metabolizing enzymes. *Drug. Metab. Rev.* **16**, 119–156
7. Massey, V., Komai, H., Palmer, G., and Elion, G.B. (1970) On the mechanism of inactivation of xanthine oxidase by allopurinol and other pyrazolo [3,4-d] pyrimidines. *J. Biol. Chem.* **245**, 2837–2844
8. Ichida, K., Yoshida, M., Sakuma, R., and Hosoya, T. (1998) Two siblings with classical xanthinuria type 1: significance of allopurinol loading test. *Intern. Med.* **37**, 77–82
9. Reiter, S., Simmonds, H.A., Zollner, N., Braun, S.L., and Knedel, M. (1990) Demonstration of a combined deficiency of xanthine oxidase and aldehyde oxidase in xanthinuric patients not forming oxipurinol. *Clin. Chim. Acta.* **187**, 221–234
10. Simmonds, H.A., Reiter, S., and Nishino, T. (1995) Hereditary xanthinuria in *The Metabolic and Molecular Bases of Inherited Disease* (Scriver, C.R., Beaudet, A.L., Sly, W.S., and Valle, D., eds.) Vol. II, 7th edn, pp. 1781–1798, McGraw-Hill Inc., USA
11. Johnson, J.L. and Wadman, S.K. (1995) Molybdenum cofactor deficiency and isolated sulfite oxidase deficiency in *The Metabolic and Molecular Bases of Inherited Disease* (Scriver, C.R., Beaudet, A.L., Sly, W.S., and Valle, D., eds.) Vol. II, 7th edn, pp. 2271–2283, McGraw-Hill Inc., USA
12. Hille, R. and Sprecher, H. (1987) On the mechanism of action of xanthine oxidase. Evidence in support of an oxo transfer mechanism in the molybdenum-containing hydroxylases. *J. Biol. Chem.* **262**, 10914–10917
13. Greenwood, R.J., Wilson, G.L., Pilbow, J.R., and Wedd, A.G. (1993) Molybdenum(V) Sites in xanthine oxidase and relevant analog complexes: comparison of oxygen-17 hyperfine coupling. *J. Am. Chem. Soc.* **115**, 5385–5392
14. Holm, R.H. (1990)) The biologically relevant oxygen atom transfer chemistry of molybdenum. *Coord. Chem. Rev.* **100**, 183–221
15. Lippard, S.J. and Berg, J.M. (1994) *Principles of Bioinorganic Chemistry* pp. 318–324, University Science Books, Mill Vale, CA
16. Howes, B.D., Bray, R.C., Richards, R.L., Turner, N.A., Bennett, B., and Lowe, D.J. (1996) Evidence favoring molybdenum-carbon bond formation in xanthine oxidase action: 17Q- and 13C-ENDOR and kinetic studies. *Biochemistry* **35**, 1432–1443
17. Maiti, N.C., Tomita, T., Kitagawa, T., Okamoto, K., and Nishino, T. (2003) Resonance Raman studies on xanthine oxidase: observation of Mo(VI)-ligand vibrations. *J. Biol. Inorg. Chem.* **8**, 327–333
18. Xia, M., Dempski, R., and Hille, R. (1999) The reductive half-reaction of xanthine oxidase. Reaction with aldehyde substrates and identification of the catalytically labile oxygen. *J. Biol. Chem.* **274**, 3323–3330
19. Huber, R., Hof, P., Duarte, R.O., Moura, J.J., Moura, I., Liu, M.Y., LeGall, J., Hille, R., Archer, M., and Romao, M.J. (1996) A structure-based catalytic mechanism for the xanthine oxidase family of molybdenum enzymes. *Proc. Natl. Acad. Sci. USA* **93**, 8846–8851
20. Okamoto, K., Matsumoto, K., Hille, R., Eger, B.T., Pai, E.F., and Nishino, T. (2004) The crystal structure of xanthine oxidoreductase during catalysis: implications for reaction mechanism and enzyme inhibition. *Proc. Natl. Acad. Sci. USA* **101**, 7931–7936
21. Leimkuhler, S., Stockert, A.L., Igarashi, K., Nishino, T., and Hille, R. (2004) The role of active site glutamate residues in catalysis of Rhodobacter capsulatus xanthine dehydrogenase. *J. Biol. Chem.* **279**, 40437–40444
22. Ichida, K., Amaya, Y., Noda, K., Minoshima, S., Hosoya, T., Sakai, O., Shimizu, N., and Nishino, T. (1993) Cloning of the cDNA encoding human xanthine dehydrogenase (oxidase): structural analysis of the protein and chromosomal location of the gene. *Gene* **133**, 279–284
23. Waud, W.R. and Rajagopalan, K.V. (1976) Purification and properties of the NAD+-dependent (type D) and O2-dependent (type O) forms of rat liver xanthine dehydrogenase. *Arch. Biochem. Biophys.* **172**, 354–364
24. Laemmli, U.K. (1970) Cleavage of structural proteins during the assembly of the head of bacteriophage T4. *Nature* **227**, 680–685
25. Laskowski, R.A., MacArthur, M.W., Moss, D.S., and Thornton, J.M. (1993) PROCHECK: a program to check the stereochemical quality of protein structures. *J. Appl. Crystallogr.* **26**, 283–291
26. Kissinger, C.R., Gehlhaar, D.K., and Fogel, D.B. (1999) Rapid automated molecular replacement by evolutionary search. *Acta Crystallogr. D Biol. Crystallogr.* **55**, 484–491
27. Jones, T.A., Zou, J.Y., Cowan, S.W., and Kjeldgaard, M. (1991) Improved methods for building protein models in electron density maps and the location of errors in these models. *Acta Crystallogr. A* **47** (Pt 2), 110–119
28. Brunger, A.T., Adams, P.D., Clore, G.M., DeLano, W.L., Gros, P., Grosse-Kunstleve, R.W., Jiang, J.S., Kuszewski, J., Nilges, M., Pannu, N.S., Read, R.J., Rice, L.M., Simonson, T., and Warren, G.L. (1998) Crystallography & NMR system: a new software suite for macromolecular structure determination. *Acta Crystallogr. D Biol. Crystallogr.* **54**, 905–921
29. Nishino, T., Amaya, Y., Kawamoto, S., Kashima, Y., Okamoto, K., and Nishino, T. (2002) Purification and characterization of multiple forms of rat liver xanthine

oxidoreductase expressed in baculovirus-insect cell system. *J. Biochem. (Tokyo)* **132**, 597–606
30. Iwasaki, T., Okamoto, K., Nishino, T., Mizushima, J., and Hori, H. (2000) Sequence motif-specific assignment of two [2Fe-2S] clusters in rat xanthine oxidoreductase studied by site-directed mutagenesis. *J. Biochem. (Tokyo)* **127**, 771–778
31. Massey, V., Brumby, P.E., and Komai, H. (1969) Studies on milk xanthine oxidase. Some spectral and kinetic properties. *J. Biol. Chem.* **244**, 1682–1691
32. Ikegami, T. and Nishino, T. (1986) The presence of desulfo xanthine dehydrogenase in purified and crude enzyme preparations from rat liver. *Arch. Biochem. Biophys.* **247**, 254–260
33. Krenitsky, T.A., Spector, T., and Hall, W.W. (1986) Xanthine oxidase from human liver: purification and characterization. *Arch. Biochem. Biophys.* **247**, 108–119
34. Terao, M., Kurosaki, M., Demontis, S., Zanotta, S., and Garattini, E. (1998) Isolation and characterization of the human aldehyde oxidase gene: conservation of intron/exon boundaries with the xanthine oxidoreductase gene indicates a common origin. *Biochem. J.* **332** (Pt 2), 383–393
35. Enroth, C., Eger, B.T., Okamoto, K., Nishino, T., Nishino, T., and Pai, E.F. (2000) Crystal structures of bovine milk xanthine dehydrogenase and xanthine oxidase: structure-based mechanism of conversion. *Proc. Natl. Acad. Sci. USA* **97**, 10723–10728
36. Okamoto, K., Eger, B.T., Nishino, T., Kondo, S., Pai, E.F., and Nishino, T. (2003) An extremely potent inhibitor of xanthine oxidoreductase. Crystal structure of the enzyme-inhibitor complex and mechanism of inhibition. *J. Biol. Chem.* **278**, 1848–1855
37. Truglio, J.J., Theis, K., Leimkuhler, S., Rappa, R., Rajagopalan, K.V., and Kisker, C. (2002) Crystal structures of the active and alloxanthine-inhibited forms of xanthine dehydrogenase from Rhodobacter capsulatus. *Structure* **10**, 115–125
38. Nishino, T., Okamoto, K., Kawaguchi, Y., Hori, H., Matsumura, T., Eger, B.T., Pai, E.F., and Nishino, T. (2005) Mechanism of the conversion of xanthine dehydrogenase to xanthine oxidase: identification of the two cysteine disulfide bonds and crystal structure of a non-convertible rat liver xanthine dehydrogenase mutant. *J. Biol. Chem.* **280**, 24888–24894
39. Maiti, R., Van Domselaar, G.H., Zhang, H., and Wishart, D.S. (2004) SuperPose: a simple server for sophisticated structural superposition. *Nucleic Acids Res.* **32** (Web Server issue), W590–W594
40. Glatigny, A., Hof, P., Romao, M.J., Huber, R., and Scazzocchio, C. (1998) Altered specificity mutations define residues essential for substrate positioning in xanthine dehydrogenase. *J. Mol. Biol.* **278**, 431–438
41. Huh, K., Yamamoto, I., Gohda, E., and Iwata, H. (1976) Tissue distribution and characteristics of xanthine oxidase and allopurinol oxidizing enzyme. *Jpn. J. Pharmacol.* **26**, 719–724
42. Leimkuhler, S., Hodson, R., George, G.N., and Rajagopalan, K.V. (2003) Recombinant Rhodobacter capsulatus xanthine dehydrogenase, a useful model system for the characterization of protein variants leading to xanthinuria I in humans. *J. Biol. Chem.* **278**, 20802–20811
43. Bray, R.C. (1975) Molybdenum iron-sulfur flavin hydroxylases and related enzymes in *The Enzymes* (Boyer, P.D., ed.) Vol. XII, 3rd edn, part B, pp. 299–419, Academic Press, New York and London
44. Nishino, T., Ito, R., and Tsushima, K. (1975) Studies on chicken liver xanthine dehydrogenase with reference to the problem of non-equivalence of FAD moieties. *Biochim. Biophys. Acta* **403**, 17–22
45. Godber, B.L., Schwarz, G., Mendel, R.R., Lowe, D.J., Bray, R.C., Eisenthal, R., and Harrison, R. (2005) Molecular characterization of human xanthine oxidoreductase: the enzyme is grossly deficient in molybdenum and substantially deficient in iron-sulphur centres. *Biochem. J.* **388**, 501–508
46. Itoh, R., Nishino, T., Usami, C., and Tsushima, K. (1978) An immunochemical study of the changes in chicken liver xanthine dehydrogenase activity during dietary adaptation. *J. Biochem. (Tokyo)* **84**, 19–26
47. Nishino, T., Nishino, T., and Tsushima, K. (1981) Purification of highly active milk xanthine oxidase by affinity chromatography on Sepharose 4B/folate gel. *FEBS Lett.* **131**, 369–372
48. Temple, C.A., Graf, T.N., and Rajagopalan, K.V. (2000) Optimization of expression of human sulfite oxidase and its molybdenum domain. *Arch. Biochem. Biophys.* **383**, 281–287
49. Neumann, M., Schulte, M., Junemann, N., Stocklein, W., and Leimkuhler, S. (2006) Rhodobacter capsulatus XdhC is involved in molybdenum cofactor binding and insertion into xanthine dehydrogenase. *J. Biol. Chem.* **281**, 15701–15708
50. Ichida, K., Matsumura, T., Sakuma, R., Hosoya, T., and Nishino, T. (2001) Mutation of human molybdenum cofactor sulfurase gene is responsible for classical xanthinuria type II. *Biochem. Biophys. Res. Commun.* **282**, 1194–1200
51. Ichida, K., Amaya, Y., Kamatani, N., Nishino, T., Hosoya, T., and Sakai, O. (1997) Identification of two mutations in human xanthine dehydrogenase gene responsible for classical type I xanthinuria. *J. Clin. Invest.* **99**, 2391–2397